Organic-inorganic telechelic molecules: Solution properties from simulations

Alberto Striolo[a)]
School of Chemical Biological and Materials Engineering, University of Oklahoma, Norman, Oklahoma 73019

Clare McCabe
Department of Chemical Engineering, Vanderbilt University, Nashville, Tennessee 37235

Peter T. Cummings
Department of Chemical Engineering, Vanderbilt University, Nashville, Tennessee 37235 and Nanomaterials Theory Institute and Chemical Sciences Division, Oak Ridge National Laboratory, Oak Ridge, Tennessee 37831-6494

(Received 9 June 2006; accepted 10 August 2006; published online 11 September 2006)

We report molecular dynamics simulations for telechelic molecules composed of two polyhedral oligomeric silsesquioxane (POSS) cages connected by one hydrocarbon backbone dissolved in liquid normal hexane. Silsesquioxanes are novel hybrid organic-inorganic molecules that are useful as building blocks for the synthesis of nanostructured materials. By including POSS molecules within a polymeric material it is possible to modify mechanical properties such as resistance to heat and glass transition temperatures. Unfortunately, the molecular mechanisms responsible for these enhancements are at present not completely understood. In an effort to elucidate the molecular phenomena responsible for these effects, we have studied the conformation of telechelic POSS molecules in solution, as well as their self-diffusion coefficients, as a function of the length of the hydrocarbon backbone. We focus on molecules in which the radius of gyration of the alkane backbone is comparable to the size of the silsesquioxane cages. Our results indicate that the backbone has a significant influence on both the equilibrium and the transport properties of dissolved telechelic hybrid molecules. These observations are useful for developing strategies to direct the self-assembly of nanostructured materials. © *2006 American Institute of Physics*.
[DOI: 10.1063/1.2348641]

I. INTRODUCTION

The mechanical and structural features of polymers can frequently be improved with the incorporation of nanoscale particulates.[1–4] The glass transition temperature, melting point, stress-strain behavior, and microphase separation can all be altered by introducing an inorganic component into an organic polymer matrix.[5] Nanocomposite materials can be produced via top-down or bottom-up approaches. In the top-down approach the different components are blended together with the help of mechanical work and/or thermal energy; once the resulting blends are obtained, they cannot be further processed easily due to the lack of control of their microstructure. An alternative top-down approach involves cross-linking silica gel derived hybrids yielding a network of organic-inorganic hybrid polymers. In this case, the molecular structure of the final material is poorly defined due to the lack of control during the cross-linking process.[6] In the bottom-up approach one wishes to generate well-defined and monodisperse hybrid organic-inorganic building blocks that self-assemble yielding materials with well-defined structure-property characteristics;[7,8] bottom-up approaches are limited by the availability of suitable building blocks and an understanding of how constituent structure and interactions impact the final materials properties.

Hybrid organic-inorganic polyhedral oligomeric silsesquioxanes[9] (POSSs) show promising features that allow them to be employed not only as additives,[10–12] but also as nanobuilding blocks for the synthesis of supramolecular composite materials.[13–15] Enhanced properties of POSS-based hybrid copolymers include increased thermal stability, higher glass transition temperature, augmented flame and heat resistance, and enhancement in the modulus and melt strengths compared to the properties of the pristine polymers.[16–18] The most studied POSS molecules are cages of silicon and oxygen with composition $Si_8O_{12}R_8$ where R is an organic group (hydrogen, alcohol, chlorosilane, epoxide, ester, isocyanate, acrylate, silane, etc.[19]). It is often possible to synthesize POSS monomers with seven organic groups bound at seven silicon atoms to provide solubility, while incorporating one reactive group at the eighth silicon atom. The reactive group can be exploited to produce, for example, random copolymers containing POSS monomers.[13–15,20] Control over the location of the POSS cages within an organic polymer is possible using living/controlled polymerization methodologies. For example, POSS monomers have

[a)]Author to whom correspondence should be addressed. Electronic mail: astriolo@ou.edu

been incorporated into linear and star polymers,[13,21,22] telechelic polymers with hydrophilic poly(ethylene oxide) backbones,[23,24] hemitelechelic macromolecules with polystyrene backbones,[25] and POSS siloxane oligomers.[26] The interest in telechelic and hemitelechelic molecules stems from the availability of hybrid systems in which the radius of gyration of the organic backbone is comparable to the radius of the POSS monomer. These materials are expected to foster a variety of novel technological applications.[18,27,28] To fully realize their potentials a detailed understanding of their structure-function properties is required. This can be achieved through synergistic experimental and molecular simulation approaches.[29–31]

As part of a larger multiscale theoretical project,[32] we have studied a number of POSS-containing systems, with particular attention on those based to the $(SiO_{1.5})_8H_8$ building block. From electronic-structure calculations we have demonstrated that by combining force fields independently developed to describe silsesquioxanes and alkanes it is possible to correctly predict the structure of isolated POSS monomers[33] as well as that of crystals composed solely of POSS monomers.[34] Using all-atom molecular dynamics simulations with a force field that offers a good compromise between molecular accuracy and economy of computational time, we predicted the potential of mean force and the diffusion coefficient of POSS monomers dissolved in a melt of short poly(dimethyl siloxane) chains[35] and of hexadecane molecules.[36] Our results demonstrated that by substituting an organic group R on each corner of the POSS cage to yield $(SiO_{1.5})_8R_8$ it is possible to significantly alter both the features of the pair potential of mean force between POSS monomers and their self-diffusion coefficient. These results are currently being employed to develop coarse-grained models to describe the formation of supramolecular structures, e.g., lamellae, and of nanostructured materials.[37] Once the all-atom simulation results are included in the formulation of coarse-grained models the theoretical predictions should become more reliable, allowing us to explain experimental results obtained from the self-assembly of, for example, amphiphilic POSS molecules,[38] POSS molecules with polyoxazoline tethers,[39] hemitelechelic POSS monomers with polystyrene backbones,[25] and octavinyl POSS.[40]

In this work, we are interested in the dilute-solution properties of organic-inorganic telechelic hybrid molecules composed of two POSS monomers functionalized at seven corners by methyl groups and connected at the eighth corner by a single alkane backbone. The chemical formula of the molecule considered is $(SiO_{1.5})_8(CH_3)_7B(SiO_{1.5})_8(CH_3)_7$, where B is the alkyl backbone. In the remainder of this manuscript we refer to these molecules as POSS-alkane hybrid molecules. In Fig. 1 we present a schematic illustration for one POSS-alkane telechelic hybrid in which the alkane backbone is composed of 20 carbon atoms. In the simulations reported below, we consider backbones whose radius of gyration is comparable to the diameter of one POSS monomer [approximately 0.85 nm (Ref. 36)]. We study these molecules, in hexane over a temperature range of 300–600 K, as prototypes of cross-linked POSS molecules in a polymer melt, both from their intrinsic interest and as part of the development of mesoscale force fields for the study of cross-linked POSS molecules in polymer solvents.

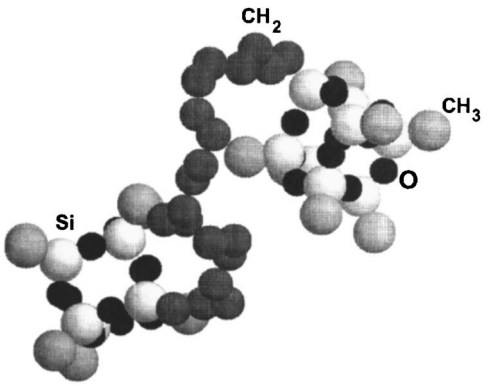

FIG. 1. Schematic representation of one POSS-alkane telechelic hybrid monomer $[(SiO_{1.5})_8(CH_3)_7B(SiO_{1.5})_8(CH_3)_7]$ considered in this work. The backbone B is composed of 20 CH_2 united-atom groups. In each POSS monomer seven silicon atoms are bound to a methyl group. The eighth silicon atom in each cage is bound to the hydrocarbon backbone.

The remainder of this paper is organized as follows: in Sec. II we present the simulation methods and details, in Sec. III we discuss our results, and in Sec. IV we summarize our conclusions.

II. SIMULATION DETAILS

A. Force fields

As in our earlier work,[35,36] the POSS monomers are described by implementing a force field originally developed to reproduce the radial distribution function of liquid poly(dimethyl siloxane).[41] The methyl groups are treated with a united-atom approach.[42] Atoms in the same POSS monomer interact with each other via short-range potentials. Bond-length fluctuations around the equilibrium separation r_0 are constrained by the bond potential,

$$V_b(r) = k_b(r - r_0)^2. \tag{1}$$

Bond-angle oscillations about the equilibrium angle θ_0 are constrained by the bond angle potential,

$$V_a(\theta) = k_a(\theta - \theta_0)^2 \tag{2}$$

and torsional-angle fluctuations ϕ are constrained by the torsional potential given by

$$V_t(\phi) = c_1[1 + \cos(\phi)] + c_2[1 - \cos(2\phi)] + c_3[1 + \cos(3\phi)]. \tag{3}$$

In Eqs. (1)–(3) V_b, V_a, and V_t are the bond length, angle, and torsional potentials, respectively; k_b,k_a, c_1, c_2, and c_3 are proportionality constants; r, θ, and ϕ are the instantaneous bond length, bond angle, and torsional angle, respectively. By implementing this force field it is possible to correctly reproduce experimental structural properties for $(SiO_{1.5})_8H_8$ and $(SiO_{1.5})_8(CH_3)_8$ POSS crystallites.[34]

The alkane backbone, composed of CH_2 groups, is modeled according to the TraPPE united-atom force field,[42] described later. In our previous work[33] we demonstrated that it is possible to predict the properties of POSS-alkane hybrid molecules by appropriately combining force fields originally derived to represent siloxanes and alkanes. To combine the force field used here to describe the POSS cages[41] and that used to describe the alkane backbone[42] we require an appropriate algebraic description for the $Si-CH_2$ bond length, the $O-Si-CH_2$ and $Si-CH_2-CH_2$ bond angles, and for the $Si-O-Si-CH_2$, $O-Si-CH_2-CH_2$, and $Si-CH_2-CH_2-CH_2$ torsional potentials. For consistency, we describe the $Si-CH_2$ bond-length fluctuations with Eq. (1) employing the parameters used to describe the $Si-CH_3$ bond, and the $O-Si-CH_2$ bond-angle oscillations with Eq. (2). To describe the $Si-CH_2-CH_2$ bond-angle fluctuations, following the COMPASS formalism,[43] we employ the algebraic expression

$$V_a(\theta) = k_a^{\mathrm{I}}(\theta - \theta_0)^2 + k_a^{\mathrm{II}}(\theta - \theta_0)^3 + k_a^{\mathrm{III}}(\theta - \theta_0)^4. \quad (4)$$

Because of the cubic structure of the POSS monomers and of the compact morphology of the POSS-alkane hybrid molecules considered here, we expect that the torsional potentials used to describe the chemical bond between the POSS monomer and the alkane backbone will not influence appreciably the properties of the system. Torsional motions are, in fact, hindered by steric interactions between the CH_3 groups at the POSS corners and the CH_2 groups in the backbone. Furthermore, electronic-structure calculations show very similar energy profiles for the $Si-CH_2-CH_2-CH_2$, torsional angle in propyl POSS and the $CH_2-CH_2-CH_2-CH_2$ torsional angle in butyl POSS, as well as for the $O-Si-CH_2-CH_2$ torsional angles in propyl-and ethyl-POSS monomers.[33] Based on these results the $Si-O-Si-CH_2$ potential was set equal to the $Si-O-Si-CH_3$ potential, and the $Si-CH_2-CH_2-CH_2$ torsion equal to that of $CH_2-CH_2-CH_2-CH_2$. To describe the $O-Si-CH_2-CH_2$ potential we chose the $CH_2-CH_2-CH_2-CH_2$ potential, with parameters set at half the original values.

In addition to intramolecular forces, Lennard-Jones 12-6 potentials describe nonbonded CH_3-CH_3, CH_3-O, CH_2-Si, and CH_3-Si repulsion and dispersive interactions,

$$u(r_{ij}) = 4\varepsilon_{ij}\left[\left(\frac{\sigma_{ij}}{r_{ij}}\right)^{12} - \left(\frac{\sigma_{ij}}{r_{ij}}\right)^{6}\right]. \quad (5)$$

Lennard-Jones 9-6 potentials describe nonbonded Si–O repulsion and dispersive interactions,

$$u(r_{ij}) = \varepsilon_{ij}\left[2\left(\frac{\sigma_{ij}}{r_{ij}}\right)^{9} - 3\left(\frac{\sigma_{ij}}{r_{ij}}\right)^{6}\right]. \quad (6)$$

In Eqs.(5) and (6) the parameters ε_{ij} and σ_{ij} have the usual meaning and r_{ij} is the distance between atoms i and j. Nonbonded interactions between atoms in the same molecule are not accounted for unless the pairs of atoms are separated by more than three bonds, consistent with many formalisms, including the TraPPE force field.[42]

Normal hexane (nC$_6$) is described by the TraPPE united atom force field for alkanes,[42] in which the CH_3 and CH_2 groups are treated as single spherical interaction sites (i.e., the hydrogen atoms are not treated explicitly). The united atoms are linked through rigid bonds with length of 0.154 nm. The fluctuations of bond angles and of dihedral angles are constrained through harmonic potentials of functional forms expressed by Eqs. (2) and (3), respectively. Nonbonded interactions between united atoms are treated within the Lennard-Jones 12-6 formalism, reported in Eq. (5). Interactions between dissimilar united atoms are determined from the Lorentz-Berthelot mixing rules. Nonbonded interactions between atoms in the same molecule are not accounted for unless the pairs of atoms are separated by more than three bonds. Nonbonded interactions between atoms belonging to POSS, the alkane backbone, and the nC$_6$ solvent are treated according to the Lennard-Jones 12-6 formalism expressed in Eq. (5) with the appropriate choice of interaction parameters.

In Table I we report the parameters required to implement the force fields used here.

B. Simulation algorithm

Classical molecular dynamics simulations are employed to study the properties of systems containing POSS-alkane hybrid molecules and nC$_6$. The systems considered are composed of one POSS-alkane hybrid and 290 nC$_6$ chains in a cubic simulation box with size of 4.0 nm. The number of nC$_6$ molecules is chosen to achieve a total density in the systems of approximately 0.67 g/cm^3, which is similar to the density of bulk liquid normal hexane at ambient conditions. When the alkane backbone is 20 carbon atom long we conducted additional simulations in a cubic box with size of 6.0 nm in which 984 nC$_6$ chains are dissolved. No appreciable differences were observed in the two cases.

To integrate the equations of motion we employ the DL-POLY (version 2.14) simulation suite[44] in the canonical (*NVT*) ensemble.[45] The temperature is controlled using the Nosé-Hoover thermostat (time constant of 1.0 ps). The integration time is 1 fs at 300 and 400 K and 0.5 fs at 500 and 600 K. Rigid bonds are maintained using the SHAKE algorithm.[46] We note that experimental studies corresponding to our simulations would likely be conducted under constant-pressure conditions. In separate work we have considered the effect of pressure on the effective pair potential between $(SiO_{1.5})_8(CH_3)_8$ POSS monomers dissolved in nC$_6$ at 300 and 400 K.[47] Because the results in the *NVT* and in the *NPT* ensembles were not significantly different from each other, we concluded that conducting our simulations in the *NVT* ensemble would be sufficient for the purposes of the present study.

The initial configurations are obtained using a Monte Carlo procedure developed to study colloid-polymer systems;[48] the POSS-alkane hybrid molecule is placed in the simulation box. The nC$_6$ chains are then grown within the simulation box using periodic boundary conditions in all directions. The building subroutine solely ensures that the connectivity between different polymer segments is respected and that different polymer segments do not overlap, either with each other, or with the hybrid molecule. The complete interatomic potentials are switched on in all the subsequent

TABLE I. Potential parameters for the molecular models employed in this work.

Bonds	r_0 (Å)	k_b [kcal/(mol Å^2)]
Si–O	1.64	350.12
Si–CH_3	1.90	189.65
Si–CH_2	1.90	189.65
Angles	θ_0 (deg)	k_θ [kcal/(mol rad^2)]
Si–O–Si	146.46	14.14
O–Si–O	107.82	94.50
O–Si–CH_3	110.69	49.97
O–Si–CH_2	110.69	49.97
CH_3–CH_2–CH_2	114.00	62.09
CH_2–CH_2–CH_2	114.00	62.09

Angles	θ_0 (deg)	k_θ^{I} [kcal/(mol rad^2)]	k_θ^{II} [kcal/(mol rad^3)]	k_θ^{III} [kcal/(mol rad^4)]
Si–CH_2–CH_2	112.67	39.52	−7.44	0.00
Dihedrals		c_1 (kcal/mol)	c_2 (kcal/mol)	c_3 (kcal/mol)
Si–O–Si–O		0.2250	0.0000	0.0000
Si–O–Si–CH_3		0.0000	0.0000	0.0100
Si–O–Si–CH_2		0.0000	0.0000	0.0100
O–Si–CH_2–CH_2		0.3527	−0.0677	0.7862
Si–CH_2–CH_2–CH_2		0.7054	−0.1355	1.5724
CH_3–CH_2–CH_2–CH_2		0.7054	−0.1355	1.5724
CH_2–CH_2–CH_2–CH_2		0.7054	−0.1355	1.5724
Nonbonded interactions		σ_{ij} (Å)		ε_{ij} (kcal/mol)
Si–Si		4.29		0.1310
O–O		3.30		0.0800
Si–O		3.94		0.0772
CH_3–CH_3		3.75		0.1947
CH_2–CH_2		3.95		0.0974
CH_3–CH_2		3.85		0.1377
Si–CH_3		3.83		0.1596
Si–CH_2		3.93		0.1093
O–CH_3		3.38		0.1247
O–CH_2		3.48		0.0854

simulation phases. The initial configurations are relaxed at 1000 K for 500 ps and then brought abruptly to the temperatures of interest. At each temperature the first 500 ps of simulation data are discarded to allow for complete equilibration. During the equilibration phase, the velocities are rescaled every 1000 time steps. The equilibration is considered sufficient when the total energy reaches a plateau. The production phase lasts 4 ns at each temperature considered. No drift in the total energy is observed during the production phase. One system configuration is stored every 500 fs. These configurations are used to obtain the averages for the results shown here. To ensure reliability of the results, we repeat the simulations at least ten times for each system. Therefore the total production time is 40 ns or more for each system considered.

From the stored configurations we compute the distance between the two POSS monomers in the POSS-alkane hybrid telechelic molecules. We consider a maximum POSS-POSS separation of 2.0 nm and calculate the probability $p(d)$ of finding the two POSS monomers at a separation $d \pm \delta d/2$ by computing

$$p(d) = \frac{f(d)}{\delta d}, \tag{7}$$

where $f(d)$ is the frequency with which the two POSS monomers are found at a separation $d \pm \delta d/2$. The length interval δd is typically 0.01 nm.

To determine the transport properties of the POSS-alkane hybrid molecules we consider the center of mass of the POSS monomers because experimentally it is easier to determine the diffusion coefficient of the POSS monomers than that of the complete hybrid molecule. To determine the diffusion coefficient D we compute the mean-square displacement, ΔR^2, of the centers of mass of the POSS monomers as a function of time and fit the simulation results to the Einstein equation,

$$D = \frac{1}{6} \lim_{t \to \infty} \frac{\Delta R^2}{dt}. \tag{8}$$

It should be emphasized that applying Eq. (8) to obtain the self-diffusion coefficient is meaningful only when the mean-

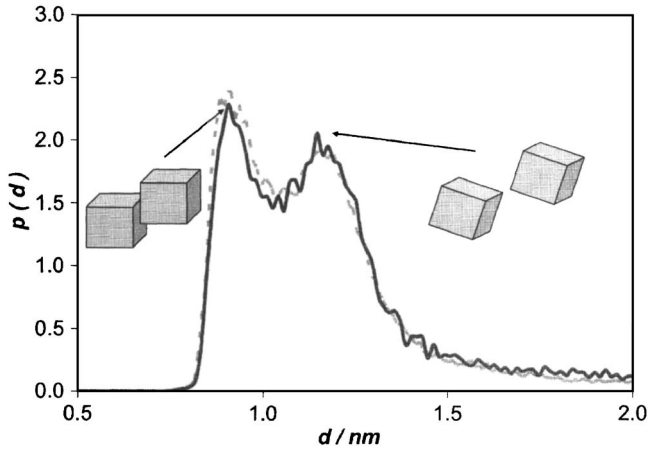

FIG. 2. Average distance between the centers of the two POSS monomers in a POSS-alkane telechelic hybrid molecule when the hydrocarbon backbone is 20 carbon atoms in length. The system temperature is 300 K. The gray dotted line represents the results obtained in a simulation box with size of 4.0 nm. The black continuous line is for the data obtained in a simulation box with size of 6.0 nm. The insets schematically illustrate the face-to-face (left) and corner-to-corner configurations (right).

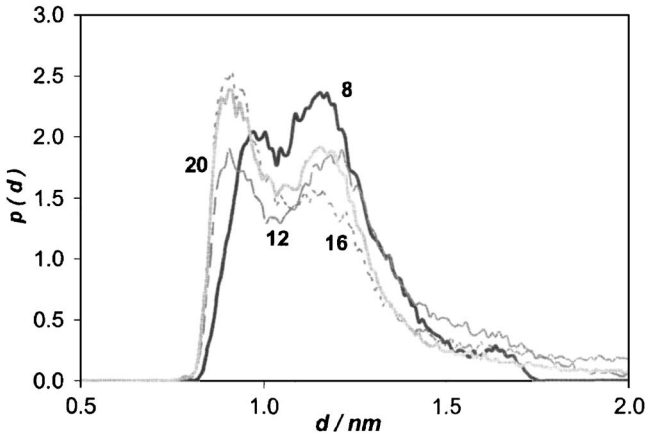

FIG. 3. Average distance between the centers of the two POSS monomers in POSS-alkane hybrid molecules at 300 K. Results are for different hydrocarbon backbones. The gray continuous line is for backbones of length 20 carbon atoms, the dotted gray line is for backbones of length 16 carbon atoms, the broken gray line is for backbones of length 12 carbon atoms, and the black continuous line is for backbones of 8 carbon atoms. In all cases the simulation box is of size 4.0 nm.

square displacement scales linearly with time, in which case Fickian-type diffusion is observed. Fickian diffusion is characterized by free random motion of the molecules considered (in our case the POSS monomers). When the motion of the molecules of interest is not free but constrained (e.g., molecules moving in narrow pores where they cannot pass each other in the direction of motion) other types of diffusion mechanisms can be observed (e.g., single-file diffusion, in which the mean-square displacement scales linearly with the square root of time).[49] In the case considered here it is not obvious that the motion of the POSS monomers is chaotic, because they are connected through the hydrocarbon backbone. Therefore it is necessary to analyze the dependence of the mean-square displacement with time. To construct the mean-square displacement we consider 20 time origins separated by 150 ps and average over the trajectories recorded for the two POSS monomers present in each system.

III. RESULTS AND DISCUSSION

A. Average POSS-POSS separation

In Fig. 2 we report the average POSS-POSS separation distance obtained for a POSS-alkane hybrid telechelic molecule in which the backbone is 20 carbon atoms in length dissolved in nC_6 at 300 K. We compare the results obtained in a simulation box with size of 4.0 nm (gray dotted line) to those obtained in a simulation box with size of 6.0 nm (black continuous line). To maintain the same nC_6 density in both systems, the number of nC_6 molecules is 290 in the smaller simulation box, and 984 in the larger one. The results shown in Fig. 2 indicate that the simulation box size has a negligible effect on the average POSS-POSS separation when the temperature is 300 K. It is expected that the size of the simulation box will affect the simulation results for longer backbones and for temperatures above 300 K, because the radius of gyration of hydrocarbons in nC_6 increases as the hydrocarbon length and/or the temperature increases. However, our results indicate that the simulation box with size of 4.0 nm is sufficiently large when the backbone is shorter than 20 carbon atoms. In the interests of computational efficiency, when the backbone is shorter than 20 carbon atoms we employ a simulation box with size of 4.0 nm for all temperatures considered. When the backbone is 20 carbon atoms long we employ a simulation box with size of 6.0 nm at temperatures higher than 300 K.

The results shown in Fig. 2 indicate that the two POSS monomers in a POSS-alkane telechelic hybrid molecule have a high probability of being at contact. The schematics in Fig. 2 illustrate the two most probable conformations for the two POSS monomers. The first peak in the average distance distribution is located at approximately 0.9 nm, which is only slightly larger than the size of one octal-methyl POSS monomer and corresponds to the "face-to-face" relative configuration between two octal-methyl POSS monomers.[36] This result is probably a consequence of the strong attraction predicted between octal-methyl POSS monomers dissolved in hydrocarbons. The presence of the hydrocarbon backbone does not seem to weaken the strong attraction between two POSS monomers dissolved in alkanes. The results shown in Fig. 2 indicate that the two POSS monomers can also be found at a center-to-center distance of approximately 1.17 nm. It is interesting to note that this corresponds to a separation between the POSS monomers in which the two monomers orient in a "corner-to-corner" configuration, where the corner of one POSS monomer is pointing in the general direction of the corner of the second POSS monomer. The "dip" in the average distance distribution observed between the two peaks at 0.9 and at 1.17 nm is probably due to the difficulty encountered by the POSS monomers to reorient from the corner-to-corner to the side-to-side relative orientations.

It is of interest to understand how the average POSS-POSS center-to-center distance changes in POSS-alkane hybrid telechelic molecules when the length of the backbone changes. In Fig. 3 we report the results obtained at 300 K

when the backbone is of length 20 (gray continuous line), 16 (gray dotted line), 12 (gray broken line), or 8 carbon atoms (black continuous line).

The results shown in Fig. 3 offer several interesting physical insights into the behavior of the POSS-alkane hybrid telechelic molecule dissolved in nC_6. As the length of the backbone decreases from 20 to 12 carbon atoms, we note that the first peak in the average POSS-POSS center-to-center distance (located at ~0.9 nm) decreases in intensity. This result could indicate that as the backbone becomes shorter it is increasingly more difficult for the two POSS monomers to find their way into a face-to-face relative orientation. We also note that the second peak, located at approximately 1.17 nm, decreases in intensity when the length of the backbone decreases from 20 to 16 carbon atoms, but then increases when the length decreases further from 16 to 12 carbon atoms. These results suggest that the length and the flexibility of the backbone have a large influence on the relative orientation, as well as on the average center-to-center separation, between the two POSS monomers. When the length of the backbone is decreased to 8 carbon atoms the behavior of the hybrid molecule changes quite significantly. We note that the first peak in the average distance distribution is shifted from 0.9 nm to approximately 0.98 nm. This result is probably a consequence of the increasing rigidity of the hydrocarbon backbone as the length of the hydrocarbon chain decreases. Our results also indicate that, for POSS-alkane telechelic hybrid molecules with backbones of 8 carbon atoms, it is more probable to find the two POSS monomers at a center-to-center separation of 1.16 nm than it is to find them at closer separations. We again interpret this result as a consequence of the increased rigidity of the backbone; it is difficult to fold the short alkane backbone enough to bring the two POSS monomers into contact with each other. The qualitative interpretation of the results presented in Fig. 3 suggests that two opposite forces act between the POSS monomers in the POSS-alkane hybrid molecule. In our previous work we predicted an effective attraction between POSS monomers dissolved in hydrocarbons.[36] We now additionally observe an effective repulsion, due to the presence of the hydrocarbon backbone. Our results indicate, as we might expect, that the repulsion becomes stronger as the length of the backbone decreases. The balance between the two forces, one attractive and the other repulsive, determines the average POSS-POSS separation reported in Fig. 3. Solvation effects such as depletion interactions could also come into play, especially at close POSS-POSS separations. If present, depletion forces would introduce additional attractive interactions between the two POSS monomers.[50] To test this possibility we have performed simulations in which the two POSS monomers are kept at a fixed center-to-center separation in the corner-to-corner orientation with the alkane backbone bound to the closest corners of the two POSS monomers. During the course of the simulation we monitored the average density of the nC_6 monomers in the vicinity of the two POSS monomers, following a procedure similar to that used in our previous work on the interaction between colloidal nanoparticles dissolved in nonadsorbing polymer solutions.[48] We considered a plane that contains the centers of the two POSS monomers, and calculated the density of nC_6 segments in small squares of volume 0.000 064 nm^3 located on the plane. In Fig. 4 we report the average density of the nC_6 monomers around the interacting POSS monomers linked by hydrocarbon backbones. We report data for POSS monomers maintained at separations of 0.99 nm (top panels) and 1.29 nm (bottom panels). Results are for POSS-alkane hybrid telechelic molecules with backbones of length 12 (left) and 20 (right) carbon atoms. Similar results were obtained for POSS-alkane hybrid telechelic molecules with backbones of 16 carbon atoms, but those results are not shown here for clarity. The simulations are conducted at 500 K because we expect the depletion effect, if present, to be stronger at higher temperatures. From the figures, it is interesting to note that the solvent monomers instead of being depleted accumulate near the POSS monomers and appear to form a "shell" around them. This is probably a consequence of the methyl groups bound to the silicon atoms in the POSS monomers, which are chemically similar to the nC_6 molecules and therefore attract them. The region of high solvent density around the POSS monomers is surrounded by a depletion region in which the solvent density is less than that in the bulk. In all the cases considered there is also an accumulation of solvent between the points of closest contact between the two POSS monomers. This is probably a consequence of the attraction between the alkane backbone and the nC_6 solvent molecules. The difficulty encountered in displacing the solvent molecules that accumulate near the POSS monomers may be responsible for the dip in the average POSS-POSS center-to-center distance reported at distances between 0.9 and 1.17 nm (see Fig. 2). It is also interesting that the length of the backbone does not influence these results.

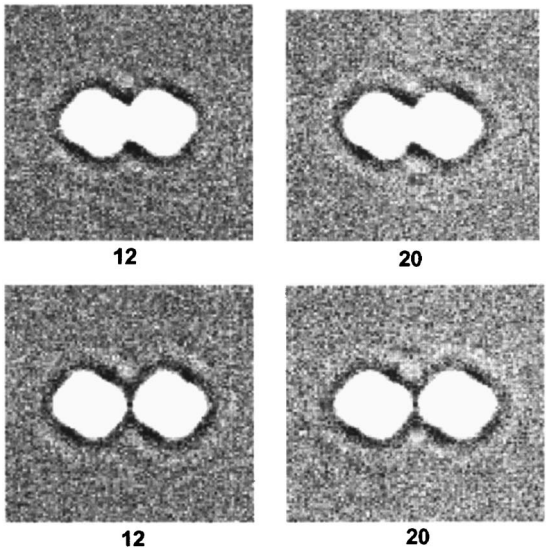

FIG. 4. Average density distribution for the nC_6 monomers (either CH_3 or CH_2 groups) around the POSS monomers. The top figures are for POSS monomers maintained at a fixed center-to-center separation of 0.99 nm, whereas the bottom figures are for POSS monomers maintained at a fixed separation of 1.29 nm. White indicates 0 segments/nm^3, and black ~45 segments/nm^3. From left to right results are for POSS-alkane hybrid molecules with backbone of lengths 12 and 20 carbon atoms. Results are obtained at 500 K. In all cases, the simulation box size is 4.0 nm.

We have also investigated the effect of temperature on

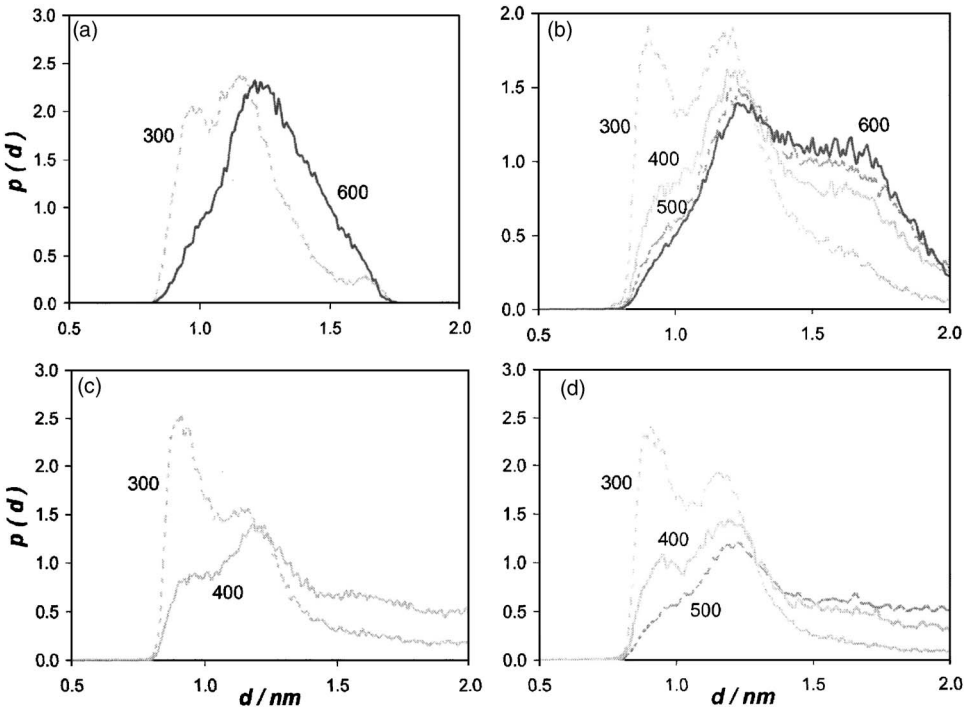

FIG. 5. Average POSS-POSS center-to-center distance for POSS-alkane hybrid molecules with backbones of 8 (panel A), 12 (panel B), 16 (panel C), and 20 carbon atoms (panel D). Results are obtained at 300 K (light dotted gray lines), 400 K (continuous gray lines), 500 K (dark dotted gray lines), and 600 K (black continuous lines). The simulation box size is 4.0 nm for the results shown in panels A, B, and C; and 6.0 nm for the results shown in panel D.

the average POSS-POSS center-to-center separation. In Fig. 5 we show the results obtained for POSS-alkane hybrid telechelic molecules with backbones of length 8 (panel A), 12 (panel B), 16 (panel C), or 20 carbon atoms (panel D) at 300 (light dotted gray lines), 400 (continuous gray lines), 500 (dark dotted gray lines), and 600 K (black continuous lines). Our results indicate that temperature has a strong effect on the average POSS-POSS center-to-center distance. Results obtained for POSS-alkane hybrid telechelic molecules with backbones of 12 and 20 carbon atoms (panels B and D, respectively) indicate that the average POSS-POSS distance changes significantly when the temperature is increased from 300 to 400 K, but it changes only minimally as the temperature increases from 400 to 500 and 600 K. When the hydrocarbon backbone is composed of at least 12 carbon atoms our results indicate that as the temperature increases from 300 to 400 K the first peak, located at approximately 0.9 nm at 300 K, decreases significantly in intensity and becomes a shoulder in the average POSS-POSS center-to-center distance plot. On the contrary, the second peak, located at approximately 1.25 nm, remains quite pronounced, even when the temperature is increased above 400 K. The data indicate that as the temperature increases it becomes more and more probable to observe the two POSS monomers at center-to-center separations above 1.25 nm, which is expected because as the temperature increases the thermal motion increases and the effective attraction between octalmethyl POSS monomers dissolved in hydrocarbons decreases.[36] The maximum separation at which the two POSS monomers can be observed from each other is determined by the length of the hydrocarbon backbone. In particular, we observe that in the case of a backbone of 8 carbon atoms in length (panel A in Fig. 5) the two POSS monomers are not seen at a center-to-center separation larger than 1.75 nm, even when the temperature is increased to 600 K. We observe that the effect of temperature on the features of the average POSS-POSS center-to-center separation is more pronounced as the length of the backbone increases. In particular, when the backbone is 20 carbon atoms in length (panel D in Fig. 5) we observe that the first peak (located at approximately 0.9 nm at 300 K) becomes weaker at 400 K, and is nothing but a slightly perceivable shoulder at 500 K. The second peak (located at approximately 1.25 nm at 300 K) becomes progressively weaker as the temperature increases, whereas when the backbone is of 12 carbon atoms in length, little change is observed when the temperature is increased above 400 K, within the accuracy of our calculations.

The POSS-alkane hybrid telechelic molecules with a backbone of 8 carbon atoms in length manifest a surprisingly different behavior. It appears that as the temperature is increased to 600 K the two POSS monomers are not found at a separation of approximately 0.98 nm. In other words, the first peak, while strong at 300 K, disappears almost completely at 600 K. The second peak is shifted from approximately 1.2 nm at 300 K to approximately 1.3 nm at 600 K. As the temperature increases the thermal motion of the backbone prevents the POSS monomers from coming together in the face-to-face conformation, and due to the short length of the backbone, the two POSS monomers are not found at distances larger than 1.75 nm from each other.

To appreciate the effect of the backbone length on the average POSS-POSS center-to-center separation at higher temperatures, we report in Fig. 6 the results obtained at 400 K when the backbone is of length 20 (gray continuous line), 16 (gray dotted line), or 12 carbon atoms (black continuous line). Surprisingly, we note that the average separation in the three cases is almost identical when we consider the statistical uncertainty in our calculations. The main difference between the results shown in Fig. 6 is that when the

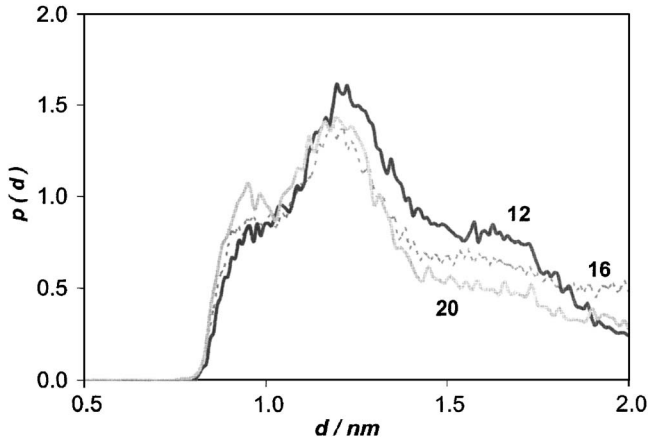

FIG. 6. Average distance between the centers of the two POSS monomers at 400 K. Results are for different hydrocarbon backbones. The gray continuous line is for backbones of length 20 carbon atoms, the dotted gray line is for backbones of length 16 carbon atoms, and the black continuous line is for backbones of 12 carbon atoms. The simulation box is of size 4.0 nm when the backbone is of length 12 or 16 carbon atoms, and 6.0 nm when the backbone is 20 carbon atoms in length.

backbone is of 12 carbon atoms in length, the peak at approximately 1.3 nm is slightly higher than those observed for longer backbones, and that the probability to observe the two POSS monomers at distances larger than approximately 1.8 nm decreases faster when the backbone is 12 carbon atoms in length than it does for longer backbones. We also observe that the shoulder at a POSS-POSS center-to-center separation of approximately 0.9 nm is slightly more pronounced for the longer backbone considered, probably because the length of the hydrocarbon chain permits the backbone to be more flexible; thus the POSS-POSS repulsion due to the rigidity of the backbone is less intense compared to that observed for shorter backbones.

B. Self-diffusion coefficient

As mentioned earlier, to assess the transport properties of the POSS-alkane hybrid molecules we have determined the mean-square displacement of the POSS monomers. Given the results shown for the average POSS-POSS center-to-center separation we expect that the differences in behavior between the POSS-alkane hybrid telechelic molecules with backbones of different lengths will be more evident at 300 K than at higher temperatures. Therefore we concentrate on the results obtained at room temperature. As mentioned earlier, it is of interest to understand if the diffusion mechanism is Fickian, so that we can apply Eq. (8) to obtain the self-diffusion coefficients from the mean-square displacement results. In Fig. 7 we report representative mean-square displacements as a function of time for POSS monomers in POSS-alkane hybrid molecules with backbones of 8 (panel A), 12 (panel B), 16 (panel C), or 20 carbon atoms (panel D). The results shown in Fig. 7 indicate that the mean-square displacement is approximately a linear function of time, thus suggesting that diffusion occurs through a Fickian mechanism. In the case of a backbone of 16 carbon atoms, our results indicate that the slope changes after a lag time that lasts up to several hundred picoseconds. The change in slope may be an indication of the presence of two diffusion mechanisms for the POSS monomers in POSS-alkane telechelic hybrid molecules. It is possible that at short times the motion of the two POSS monomers is strongly coordinated, because of the presence of the hydrocarbon backbone that connects the monomers. However, after a lag time that presumably depends on the length of the backbone, the motion becomes Fickian and the self-diffusion coefficient can be estimated by using Eq. (8). However, we should point out that the data presented in Fig. 7 are not enough to corroborate these latter speculations, particularly when one observes that in 1 ns of simulation time the center of mass of the POSS monomers never travels further than 2 nm. Longer production runs would be necessary to corroborate our speculations, although we point out that the results discussed here were obtained as average of at least ten independent simulation runs each comprosed of 4 ns of production time.

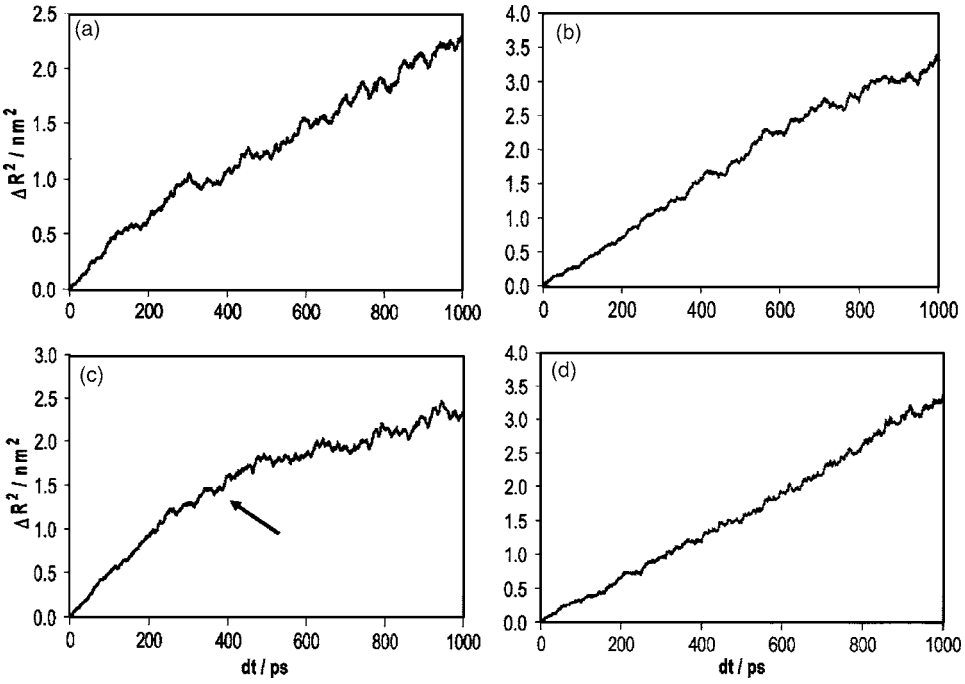

FIG. 7. Representative mean-square displacement for the POSS monomers of POSS-alkane hybrid molecules dissolved in nC_6 at 300 K. Different panels represent the results obtained for hybrid molecules with backbones of different lengths. Panel A is for backbone of length 8 carbon atoms, panel B is for 12 carbon atoms, panel C is for 16 carbon atoms, and panel D is for backbone of length 20 carbon atoms. In all cases the simulation box is of size 4.0 nm. The arrow in panel C indicates the change in slope observed for the mean-square displacement as a function of time.

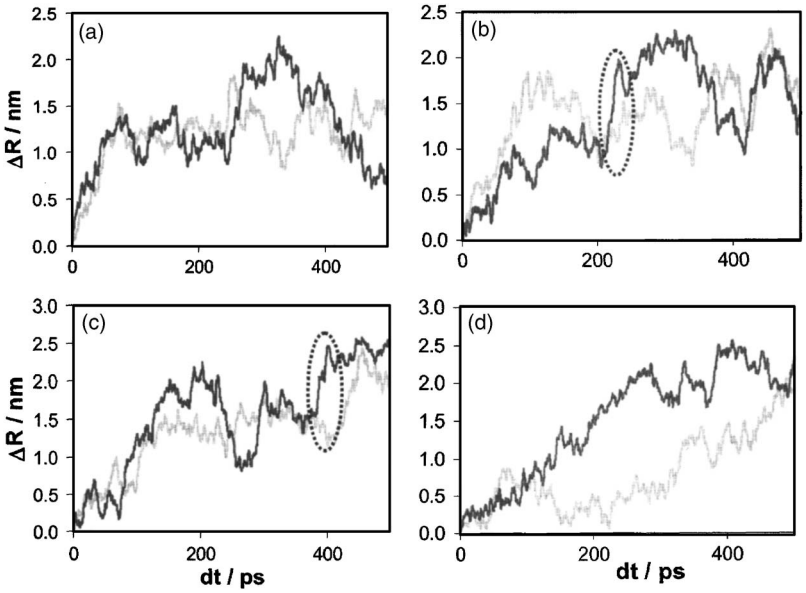

FIG. 8. Representative displacements for the two POSS monomers of POSS-alkane hybrid molecules dissolved in nC$_6$ at 300 K. Panel A is for backbone of length 8 carbon atoms, panel B is for 12 carbon atoms, panel C is for 16 carbon atoms, and panel D is for backbone of length 20 carbon atoms. In all cases the simulation box is of size 4.0 nm. The circles in panels B and C highlight the events in which one POSS monomer travels more than 0.5 nm in a very short period of time.

To assess the mechanism of motion we have monitored the displacement of each POSS monomer as a function of time. The procedure is explained in detail in a previous publication.[35] In Fig. 8 we report representative displacements as a function of time for two POSS monomers (linked by the hydrocarbon backbone) when the backbone is of length 8, 12, 16, or 20 carbon atoms. The results shown in Fig. 8 suggest several interesting features. As expected, when the backbone is 8 carbon atoms in length (panel A) the motion of the two POSS monomers is highly coordinated. Our results suggest that when one monomer moves, the second often repeats the same movement after a short period of time. This is clearly due to the short backbone that keeps the two POSS monomers at short distances from each other (see Fig. 3), and consequently the two POSS monomers move almost simultaneously. When the backbone is of length 12 (panel B) or 16 carbon atoms (panel C), the motion of the two POSS monomers is still somewhat coordinated, but not as much as for the shorter backbone. Although the results shown in panels B and C (backbones of 12 and 16 carbon atoms in length, respectively) suggest that from time to time it is possible to observe fast movements for one POSS monomer (see dotted circles), they do not support the existence of hopping events, which are typically observed when small molecules are dissolved in polymeric systems, and are due to density fluctuations within the polymeric matrix.[51–53]

Both the mean-square displacement results shown in Fig. 7 and the displacements shown in Fig. 8 suggest that the diffusion of the POSS monomers is Fickian at long time scales. Consequently, Eq. (8) can be used to estimate the self-diffusion coefficients.

In Fig. 9 we report our results for the self-diffusion coefficients calculated for the POSS monomers in POSS-alkane hybrid molecules in nC$_6$ at 300 K when we consider the limit at large time of the mean-square displacement results (see Fig. 7). The diffusion coefficients shown in Fig. 9 are obtained as the average of at least ten independent simulation runs, in each of which the production phase lasts 4 ns. The error bars were obtained as 1 standard deviation from the mean. Despite the length of our simulations we note that the error bars are significant and that because of the large error bars the diffusion coefficients seem almost independent on the length of the backbone. Despite the large error bars, we observe that the self-diffusion coefficients are of the same order of magnitude as those obtained for octal-methyl POSS monomers dissolved in hexadecane at 400 K.[36] Focusing on the mean value of the diffusion coefficients shown in Fig. 9, it is interesting to observe that the self-diffusion coefficient for the POSS monomers is approximately 1.2×10^{-9} m^2/s when the backbone is of length 8 carbon atoms. It then decreases as the backbone length increases to 12 and 16 carbon atoms, but increases as the backbone length reaches 20 carbon atoms. The self-diffusion coefficient is expected to decrease as the backbone length increases, because the alkane motion is hindered by its length. However, as shown in Fig. 3, we note that when the backbone is short the two POSS monomers are preferentially in contact with each other, and the POSS-alkane hybrid molecule becomes globular and it probably encounters difficulties in moving through the nC$_6$ solvent. When the backbone is only 8 carbon atoms in length, the molecule is clearly compact, as indicated by both the average POSS-POSS distance (Fig. 3) and the displace-

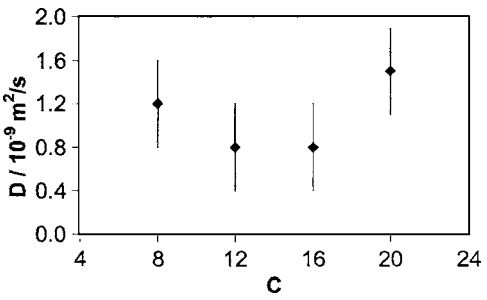

FIG. 9. Self-diffusion coefficient for the POSS monomers in POSS-alkane hybrid molecules dissolved in nC$_6$ at 300 K as a function of the number of carbon atoms in the hydrocarbon backbone (C). In all cases the simulation box is of size 4.0 nm. The error bars are calculated as 1 standard deviation from the mean value.

ment of the two POSS monomers (Fig. 8), and therefore moves quite easily through the solvent. When the backbone is slightly longer (12 or 16 carbon atoms), the two POSS monomers are attracted to each other, but they are not always at contact (see Fig. 3). Because the molecule is not compact, it encounters more hindrance to movement from the presence of the solvent, and the self-diffusion coefficient is at its minimum. When the backbone is long (20 carbon atoms), the two POSS monomers are relatively far from each other (see Fig. 3) which ensures faster self-diffusion coefficients compared to both the compact POSS-alkane hybrid molecules with 8 carbon atoms in the backbone, and to the less compact hybrid telechelic molecules with backbones of 12 or 16 carbon atoms in length.

IV. SUMMARY

We have reported molecular dynamics simulation results for telechelic hybrid organic-inorganic molecules in which two POSS monomers are bound to each other through a hydrocarbon backbone. The hybrid molecules are dissolved in liquid normal hexane at infinitely dilute concentration. We monitor the distance between the two POSS monomers as a function of the length of the hydrocarbon backbone. Simulations are conducted in the temperature range of 300–600 K. We also monitor the transport mechanism and the self-diffusion coefficient for the POSS monomers.

Our results indicate that the two POSS monomers are preferentially located in the vicinity of each other at 300 K, while they can be separated as the temperature increases. Interestingly, it is more probable to find the two POSS monomers at larger separations when the backbone is short (8 carbon atoms) than when it is long (20 carbon atoms). These results are the consequence of two different interaction mechanisms that take place between the two tethered POSS monomers. Firstly, as shown in our earlier work, POSS monomers dissolved in alkanes strongly attract each other, and secondly the presence of the backbone induces an effective repulsion between the two POSS monomers which is due to the rigidity of the backbone. This effect is stronger for short backbones, and becomes negligible for backbones with more than 16–20 carbon atoms.

The motion of the POSS monomers depends strongly on the length of the backbone. When the backbone is short the hybrid telechelic molecule is globular and the two POSS monomers move simultaneously through the solvent molecules. When the backbone is long, the motion of each POSS monomer is predominantly independent from the other. When the backbone is of intermediate length, the presence of the POSS monomers hinders the diffusion of the hybrid molecule, and the self-diffusion coefficient is very slow.

The results reported here are useful for improving our understanding of composite nanomaterials, and to facilitate the development and implementation of coarse-grained models that will allow us to understand, predict, and design the self-assembly of nanoscale building blocks yielding nanostructured materials of practical interest.

ACKNOWLEDGMENTS

The authors acknowledge financial support from the US National Science Foundation under Contract No. DMR-0103399. One of the authors (A.S.) thankfully acknowledges partial financial support from the Vice President for Research at the University of Oklahoma through a Junior Faculty Research Program Award. Calculations were performed on the VAMPIRE cluster at Vanderbilt University.

[1] E. P. Giannelis, Adv. Mater. (Weinheim, Ger.) **8**, 29 (1996).
[2] P. C. LeBaron, Z. Wang, and T. Pinnavaia, Appl. Clay Sci. **15**, 11 (1999).
[3] G. Tsagaropolous and A. Eisenberg, Macromolecules **28**, 6067 (1995).
[4] J. P. Paxton, E. D. Mowles, D. Eric, C. M. Lukehart, and A. J. Witzig, Proceedings of the American Society for Composites, 16th Technical Conference, 2001, p. 565.
[5] T. J. Pinnavaia and G. W. Beal, *Polymer Clay Nanocomposites* (Wiley, New York, 2001); Y. Kojima, A. Usuki, M. Kawasumi, A. Okada, T. Kurauchi, and O. Kamigaito, J. Polym. Sci., Part A: Polym. Chem. **31**, 1755 (1993).
[6] J. Y. Wen and G. L. Wilkes, Chem. Mater. **8**, 1667 (1996).
[7] J. Pyun, K. Matyjaszewski, J. Wu, G. M. Kim, S. B. Chun, and P. T. Mather, Polymer **44**, 2739 (2003).
[8] J. E. Riggs, Z. X. Guo, D. L. Carroll, and Y. P. Sun, J. Am. Chem. Soc. **122**, 5879 (2000); T. Song, S. Dai, K. C. Tam, S. Y. Lee, and S. H. Goh, Langmuir **19**, 4798 (2003).
[9] POSS is a trademark of Hybrid Plastics, www.hybridplastics.com
[10] B. X. Fu, L. Yang, R. H. Somani, S. X. Zong, B. S. Hsiao, S. Phillips, R. Blanski, and P. Ruth, J. Polym. Sci., Part B: Polym. Phys. **39**, 2727 (2001).
[11] E. T. Kopesky, T. S. Haddad, R. E. Cohen, and G. H. Mckinley, Macromolecules **37**, 8992 (2004).
[12] M. Joshi and B. S. Butola, Polymer **45**, 4953 (2004).
[13] J. Pyun, K. Matyjaszewski, J. Wu, G.-M. Kim, S. B. Chun, and P. T. Mather, Polymer **44**, 2739 (2003).
[14] H. Xu, J.-W. Kuo, J.-S. Lee, and F.-C. Chang, Macromolecules **35**, 8788 (2002).
[15] L. Zheng, R. J. Farris, and E. B. Coughlin, Macromolecules **34**, 8034 (2001).
[16] T. Cassagneau and F. Caruso, J. Am. Chem. Soc. **124**, 8172 (2002).
[17] K. Maka, H. Itoh, and Y. Chujo, Nano Lett. **2**, 1183 (2002).
[18] S. H. Phillips, T. S. Haddad, and S. J. Tomczak, Curr. Opin. Solid State Mater. Sci. **8**, 21 (2004).
[19] E. G. Shockey, A. G. Bolf, P. F. Jones, J. J. Schwab, K. P. Chaffee, T. S. Haddad, and J. D. Lichtenhan, Appl. Organomet. Chem. **13**, 311 (1999).
[20] J. D. Lichtenhan, N. Q. Vu, J. A. Carter, J. W. Gilman, and F. J. Feher, Macromolecules **26**, 2141 (1993); J. D. Lichtenhan, Y. A. Otonari, and M. J. Carr, *ibid.* **28**, 8435 (1995); T. S. Haddad, B. D. Viers, and S. H. Phillips, J. Inorg. Organomet. Polym. **11**, 155 (2001); P. T. Mather, H. G. Jeon, A. Romo-Uribe, T. S. Haddad, and J. D. Lichtenhan, Macromolecules **32**, 1194 (1999); L. Zheng, R. J. Farris, and E. B. Coughlin, *ibid.* **34**, 8034 (2001).
[21] J. Pyun and K. Matyjaszewski, Macromolecules **33**, 217 (1999).
[22] J. Huang, X. Li, T. Lin, C. He, K. Y. Mya, Y. Xiao, and J. Li, J. Polym. Sci., Part B: Polym. Phys. **42**, 1173 (2004).
[23] B.-S. Kim and P. T. Mather, Macromolecules **35**, 8378 (2002).
[24] R. Knischka, F. Dietsche, R. Hanselmann, H. Frey, R. Mulhaupt, and P. J. Lutz, Langmuir **15**, 4752 (1999).
[25] G. Cardoen and E. B. Coughlin, Macromolecules **37**, 5123 (2004).
[26] S. E. Anderson, C. Mitchell, T. S. Haddad, A. Vij, J. J. Schwab, and M. T. Bowers, Chem. Mater. **18**, 1490 (2006).
[27] H. P. Wu, Y. Q. Hu, K. E. Gonsalves, and M. J. Yacaman, J. Vac. Sci. Technol. B **19**, 851 (2001); S. Xiao, M. Nguyen, X. Gong, Y. Cao, H. B. Wu, O. Moses, and A. J. Heeger, Adv. Funct. Mater. **13**, 25 (2003).
[28] A. J. Waddon, L. Zheng, R. J. Farris, and E. B. Coughlin, Nano Lett. **2**, 1149 (2002).
[29] J. Choi, A. F. Yee, and R. M. Laine, Macromolecules **36**, 5666 (2003).
[30] R. K. Bharadwaj, R. J. Berry, and B. L. Farmer, Polymer **41**, 7209 (2000).
[31] F. M. Capaldi, G. C. Rutledge, and M. C. Boyce, Macromolecules **38**, 6700 (2005).
[32] C. McCabe, S. C. Glotzer, J. Kieffer, M. Neurock, and P. T. Cummings, J. Comput. Theor. Nanosci. **1**, 265 (2004).

[33] H.-C. Li, C. McCabe, A. Striolo, P. T. Cummings, C.-Y. Lee, and M. Neurock, J. Phys. Chem. A (submitted).
[34] T. C. Ionescu, F. Qi, C. McCabe, A. Striolo, J. Kieffer, and P. T. Cummings, J. Phys. Chem. B **110**, 2502 (2006).
[35] A. Striolo, C. McCabe, and P. T. Cummings, J. Phys. Chem. B **109**, 14300 (2005).
[36] A. Striolo, C. McCabe, and P. T. Cummings, Macromolecules **38**, 8950 (2005).
[37] M. H. Lamm, T. Chen, and S. C. Glotzer, Nano Lett. **3**, 989 (2003); Y.-S. Sheng, W.-J. Lin, and W.-C. Chen, J. Chem. Phys. **121**, 9693 (2004); E. R. Chan, X. Zhang, C.-Y. Lee, M. Neurock, and S. C. Glotzer, Macromolecules **38**, 6168 (2005).
[38] R. Knischka, F. Dietsche, R. Hanselmann, H. Frey, R. Mulhaupt, and P. J. Lutz, Langmuir **15**, 4752 (1999).
[39] K. M. Kim, D. K. Keum, and Y. Chujo, Macromolecules **36**, 867 (2003).
[40] C. X. Zhang, F. Babonneau, C. Bonhomme, R. M. Laine, C. L. Soles, H. A. Hristov, and A. F. Yee, J. Am. Chem. Soc. **120**, 8380 (1998).
[41] A. L. Frischknecht and J. G. Curro, Macromolecules **36**, 2122 (2003).
[42] M. G. Martin and J. I. Siepmann, J. Phys. Chem. B **102**, 2569 (1998).
[43] H. Sun, Macromolecules **28**, 701 (1995).
[44] W. Smith and T. Forester, J. Mol. Graphics **14**, 136 (1996).
[45] M. P. Allen and D. J. Tildesley, *Computer Simulation of Liquids* (Oxford University Press, New York, 1987).
[46] T. Darden, D. York, and L. Pedersen, J. Chem. Phys. **98**, 10089 (1993).
[47] A. Striolo, C. McCabe, and P. T. Cummings (unpublished).
[48] A. Striolo, C. M. Colina, N. Elvassore, K. E. Gubbins, and L. Lue, Mol. Simul. **30**, 437 (2004).
[49] A. Striolo, Nano Lett. **6**, 633 (2006).
[50] S. Asakura and F. Oosawa, J. Chem. Phys. **22**, 1255 (1954).
[51] F. Müller-Plathe, J. Chem. Phys. **94**, 3192 (1991).
[52] F. Müller-Plathe, S. C. Rogers, and W. F. van Gunsteren, Chem. Phys. Lett. **199**, 237 (1992).
[53] M. Doxastakis, D. N. Theodorou, G. Fytas, F. Kremer, R. Faller, F. Müller-Plate, and N. Hadjichristidis, J. Chem. Phys. **119**, 6883 (2003).